

# Fault Detection and Isolation in Electric Vehicle Powertrain

**Gbanaibolou Jombo<sup>1,2</sup>**

<sup>1</sup> Centre for Engineering Research, School of Physics, Engineering and Computer Science, University of Hertfordshire, UK (g.jombo@herts.ac.uk)

<sup>2</sup> Centre for Climate Change Research (C3R), School of Physics, Engineering and Computer Science, University of Hertfordshire, UK

## **Abstract**

The powertrain of an electric vehicle (EV) consists mainly of the battery, electric motor and power electronics. The safe and reliable operation of the electric vehicle depends on their fault-free operation. Fault detection and isolation methods work on the premise that small changes as a result of faults affecting a system causes variation in its operational response. This property can be used for the detection of such faults and their severity. This chapter discusses methods for detection and isolation of faults in electric vehicle powertrain components. Powertrain configuration and technologies are identified. Battery technology such as Lithium-ion batteries have gained a significant application as energy storage source in electric vehicles due to their high energy and power density, long lifespan, and low self-discharge performance under extreme temperatures. Model-based approaches are discussed for the determination of battery state of charge, state of health and effect of accelerated degradation. Fault detection in electric motor is considered. Brushless asynchronous induction motor, brushed externally excited synchronous motor and brushless permanent magnet synchronous motor are the options adopted for the electric vehicle powertrain. Signal processing-based approach such as the motor current signature analysis is explored for detection of broken rotor bar, shorten stator windings, air gap eccentricity, bearing failure and load variation effects. Lastly, fault detection in power electronics is explored. Electric vehicle electric components need complex electronics to control them. These come in the form of a power electronics module (PEM), and an inverter, which can be integral with the PEM or the electric motor itself. Inverters provide the interface between an alternating current electric component and the direct current battery. The current focus for electric vehicle power electronics is controllable solid-state switches such as insulated gate bipolar transistor. For these power drives,

the major faults are: open switch fault and short switch fault. Signal processing-based approaches are considered for detection of these faults.

**Keywords:** electric vehicle fault diagnosis, battery fault diagnosis, electric motor fault diagnosis, power electronics fault diagnosis

## **1.0 Introduction**

An electric vehicle (EV) is a vehicle that is powered, at least in part, by an electric energy source. Based on the type and combination of energy sources used in an EV, the following configurations are widely adopted: battery electric vehicle (BEV), fuel cell electric vehicle (FCEV) and hybrid-electric vehicle (HEV) [1,2]. The story of the EV is one of re-birth. EV's first came into prominence during 1897-1900, where they secured 28% of the automotive vehicle market; however, they met their demise in favour of the internal combustion engine (ICE) vehicle due to low oil prices [1,3]. In recent times, the tide has turned in favour of the EV, due mainly to government legislation on the impact on climate change from greenhouse gas emission from fossil-fuel-based ICE vehicles. As governments and industry alike craft a roadmap for decarbonising the transport sector by 2030, the EV would play an important role in achieving this. As such, the safe and reliable operation of electric vehicles becomes relevant. Fault detection and isolation (FDI) techniques provides the necessary approaches to ensure fault tolerant operation of electric vehicle powertrain components. The focus of this chapter is to review FDI techniques applied to EV powertrain components, highlighting the fundamental theories and applications.

### *1.1 EV Powertrain Configurations*

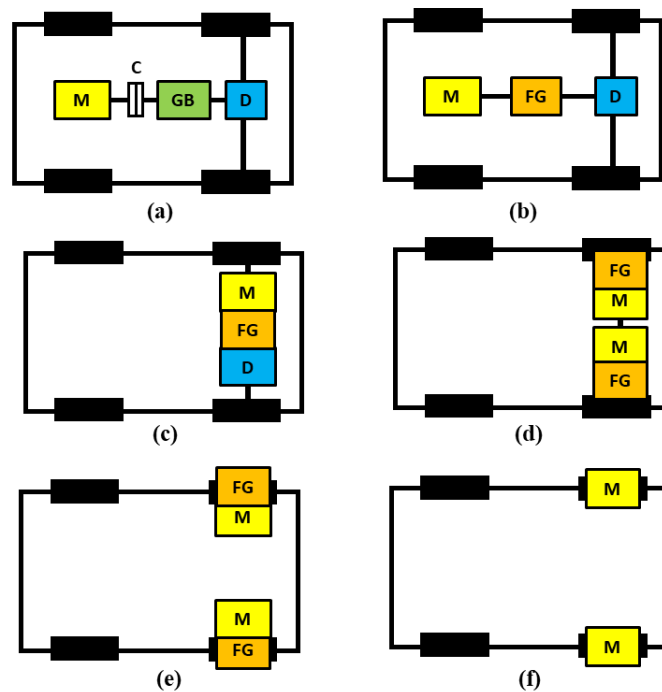
An electric vehicle powertrain can take on different configurations based on the type and combination of energy sources adopted. Basically, EV powertrain components consist of: energy source (e.g. battery, fuel cell, ICE, ultra-capacitor, flywheel), and drivetrain components that ensures the conversion of electrical energy to motive force at the wheels (i.e. electric motor and power electronics). The various combinations of these powertrain components, especially as it relates to the energy sources, leads to three broad types of EV, such as: battery electric vehicle, hybrid electric vehicle and fuel cell electric vehicle. Table 1 compares the various EV powertrain configurations.

**Table 1 Comparison of EV powertrain configurations [2]**

Types of EV	Battery EV	Hybrid EV	Fuel Cell EV
Propulsion	<ul style="list-style-type: none"> <li>Electric motor drives</li> </ul>	<ul style="list-style-type: none"> <li>Electric motor drives</li> <li>Internal combustion engines</li> </ul>	<ul style="list-style-type: none"> <li>Electric motor drives</li> </ul>
Energy system	<ul style="list-style-type: none"> <li>Battery</li> <li>Ultracapacitor</li> </ul>	<ul style="list-style-type: none"> <li>Battery</li> <li>Ultracapacitor</li> <li>ICE generating unit</li> </ul>	<ul style="list-style-type: none"> <li>Fuel cells</li> </ul>
Energy source and infrastructure	<ul style="list-style-type: none"> <li>Electric grid charging facilities</li> </ul>	<ul style="list-style-type: none"> <li>Gasoline stations</li> <li>Electric grid charging facilities (optional)</li> </ul>	<ul style="list-style-type: none"> <li>Hydrogen</li> <li>Methanol or gasoline</li> <li>Ethanol</li> </ul>
Characteristics	<ul style="list-style-type: none"> <li>Zero emission</li> <li>Independence on crude oils</li> <li>100-200 km short range</li> <li>High initial cost</li> <li>Commercially available</li> </ul>	<ul style="list-style-type: none"> <li>Very low emission</li> <li>Long driving range</li> <li>Dependence on crude oils</li> <li>Complex</li> <li>Commercially available</li> </ul>	<ul style="list-style-type: none"> <li>Zero emission or ultra-low emission</li> <li>High energy efficiency</li> <li>Independence on crude oils</li> <li>Satisfied driving range</li> <li>High cost now</li> <li>Under development</li> </ul>
Major Issue	<ul style="list-style-type: none"> <li>Battery and battery management</li> <li>High performance propulsion</li> <li>Charging facilities</li> </ul>	<ul style="list-style-type: none"> <li>Managing multiple energy sources</li> <li>Dependent on driving cycle</li> <li>Battery sizing and management</li> </ul>	<ul style="list-style-type: none"> <li>Fuel cell cost</li> <li>Fuel processor</li> <li>Fuelling system</li> </ul>

*1.1.1 Battery Electric Vehicle (BEV)*

BEV runs on the battery as the only energy source. Figure 1 shows typical configurations of BEV powertrain which can be adopted based on performance, compactness, weight, and cost requirements.



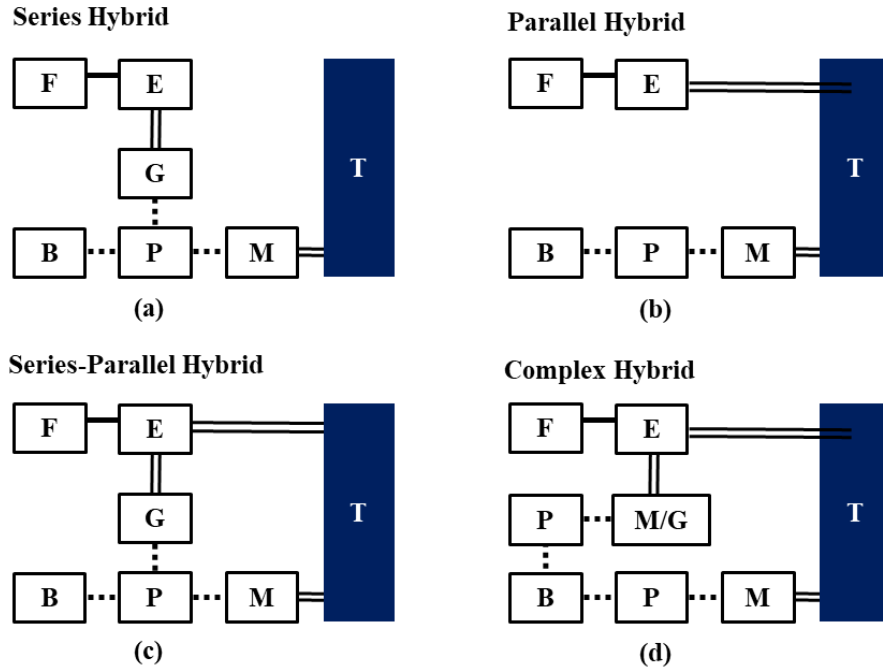
**C: Clutch, D: Differential, FG: Fixed Gearing, GB: Gearbox, M: Electric Motor**

**Figure 1 Typical BEV powertrain configurations [2]**

- a) This configuration lends itself from a converted conventional ICE powertrain for a longitudinal front engine, front wheel drive. It consist of an electric motor, clutch, gearbox and differential. This setup is heavy. Although its advantage is ability to select different gear ratio due to the presence of the clutch and gearbox. As such, high torque and low speed requirement can be meet at a low gear ratio, and low torque and high speed requirement can be meet at a higher gear ratio.
- b) This configuration reduces the weight of the BEV powertrain by replacing the clutch and gearbox with a fixed gearing. It still preserves the mechanical differential as a means to enable both drive wheels to operate a different speeds.
- c) This configuration is widely adopted by BEV. It takes the format of an integrated power assembly unit consisting of: electric motor, fixed gearing and differential. However, unlike Figure 1(b), its arrangement takes the form similar to transverse front engine, front wheel drive.
- d) This configuration eliminates the mechanical differential component with an electronic approach. It consist of dual electric motor with fixed gearing driving each wheel. The speed of each motor drive assembly can be varied electronically to achieve similar function as a mechanical differential component.
- e) This configuration represents in-wheel drivetrain. This configuration results in further reduction of powertrain weight. The motor and fixed gearing in this configuration are integral to the driving wheel. For this system, the planetary gearbox is mostly adopted due to high reduction gear ratio and inline arrangement requirements.
- f) Further simplification of the in-wheel drive is possible. This configuration eliminates the fixed gearing by adopting a low speed in-wheel electric motor. As such, vehicle speed control is tantamount to control of motor speed.

### *1.1.2 Hybrid Electric Vehicle (HEV)*

BEV is a vehicle with atleast two energy sources of which one produces electrical power [2]. This is a broad definition encompassing a variety of possible combination of energy sources. Herewith, the use of the term HEV is limited to only ICE and battery energy source combinations. Figure 2 shows typical configurations of HEV powertrain as: series hybrid, parallel hybrid, series-parallel hybrid and complex hybrid.



**B: Battery, E: ICE, F: Fuel Tank, G: Generator, M: Motor, P: Power Converter  
T: Transmission (including brakes, clutches and gears)**

**..... Electrical Link    — Hydraulic Link    == Mechanical Link**

**Figure 2 Typical HEV powertrain configuration [2]**

*a) Series hybrid:*

In this configuration, the ICE is coupled to a generator which produces electricity to either charge the battery or power the electric motor directly for electric propulsion. The series hybrid powertrain configuration is akin to an ICE-assisted EV range extender. An advantage of this configuration is the flexibility with ICE and generator placement. However, its downside is the high cost of this configuration due to the entire system, ICE and electric motor, has to be sized for maximum power output.

*b) Parallel Hybrid:*

In this configuration, both the ICE and electric motor are coupled directly to the driveshaft to provide propulsion. Herewith, the vehicle can be propelled by either ICE alone, electric motor alone or both. The parallel hybrid configuration can be viewed as an electric-assisted ICE vehicle; with an added advantage of lower emissions and fuel consumption. The advantage of a parallel hybrid configuration over the series is, only the ICE needs to be rated for maximum power output.

c) *Series-Parallel Hybrid:*

This configuration is a fusion of both the series hybrid and parallel hybrid powertrain configuration and benefits from powering option flexibility. However this flexibility comes with control system complexity and increased system configuration cost.

d) *Complex Hybrid:*

As hybrid powertrain evolves, the complex hybrid configuration accounts for such concepts that do not fit into the series hybrid, parallel hybrid and series-parallel hybrid configurations. Figure 2 (d) shows an example of a complex hybrid powertrain configuration with a bi-directional energy flow between the ICE and battery-electric motor powering option.

### *1.1.3 Fuel Cell Electric Vehicle (FCEV)*

FCEV has fuel cells as the primary energy source, and the electric motor to provide propulsion. The fuel cell can be fuelled by hydrogen or methanol. As fuel cells do not accept regenerative energy, batteries are usually included as auxiliary energy source.

## *1.2 EV Powertrain Technologies*

### *1.2.1 Energy Storage System*

Energy storage such as batteries are a vital part of the electric vehicle powertrain. The following energy storage systems are commonly used in an EV.

1) *Lithium-ion (Li-ion) Battery:*

Li-ion battery is widely adopted for EVs. They are capable of having a very high voltage and charge storage per unit mass and unit volume. Li-ion batteries can use a number of different materials as electrodes, such as lithium cobalt oxide for cathode and graphite for anode, although for portable electronic devices e.g. laptop, mobile phone, etc. For EVs, several cathode material options are possible, such as: lithium manganese oxide, lithium iron phosphate, lithium titanate, amongst others. When compared to other rechargeable battery chemistry such as Nickel-Cadmium (Ni-Cd) and Nickel Metal Hydride (Ni-MH), Li-ion has the following advantages [4]: high energy density (~100-265 Wh/kg) as shown in Figure 3, high specific power, broad useable temperature range, low maintenance (i.e. no need for

scheduled cycling to maintain battery life), no voltage depression (i.e. a memory effect artefact of a battery remembering low battery capacity due to repeated partial discharge and charging evident in Ni-Cd and Ni-MH), and low self-discharge. However, their limitations are: overheating, issues with ageing, and relatively high cost.

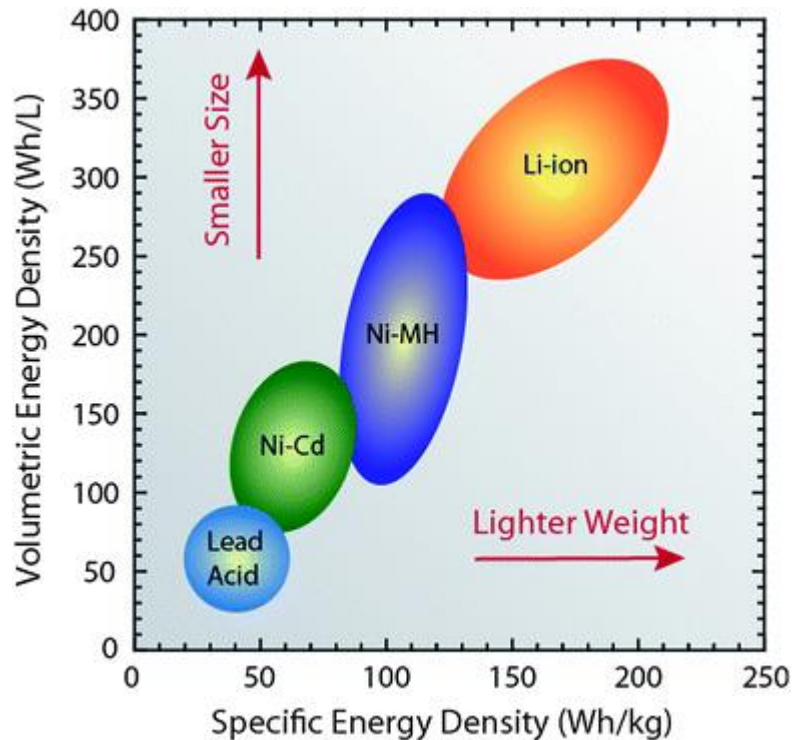


Figure 3 Comparison of battery chemistry energy density [4]

2) *Nickel Metal Hydride (Ni-MH) Battery:*

Used mostly in HEV. They have a reasonable specific power and specific energy, long useful life, and tolerant to abuse conditions. Their main limitations are: high cost, high self-discharge, poor high temperature performance, and need to control hydrogen loss.

3) *Lead Acid Battery:*

These batteries are mostly used in EV's to power auxiliary systems. They are inexpensive, they have a high specific power and tolerant to abuse conditions. The challenges with these batteries are: poor cold temperature performance, low specific energy, and poor cycle life.

4) *Ultra-Capacitor:*

The operation of ultra-capacitor is such that energy is stored in a polarised liquid between an electrode and electrolyte. They are used in EV as they provide vehicles additional power during acceleration and hill climbing as well as in recovering braking energy. They may also

be useful as secondary energy-storage devices in electric-drive vehicles because they help electrochemical batteries level load power

### 1.2.2 Electric Motor

Electric motors are the main motive component in an EV powertrain. Together with the battery, the electric motor transforms electrical energy to rotational or mechanical energy transmitted to the vehicle wheels for propulsion. Although there are various types of electric motors based on applications, the common electric motor technology applied in EV are shown in Figure 4 [3].

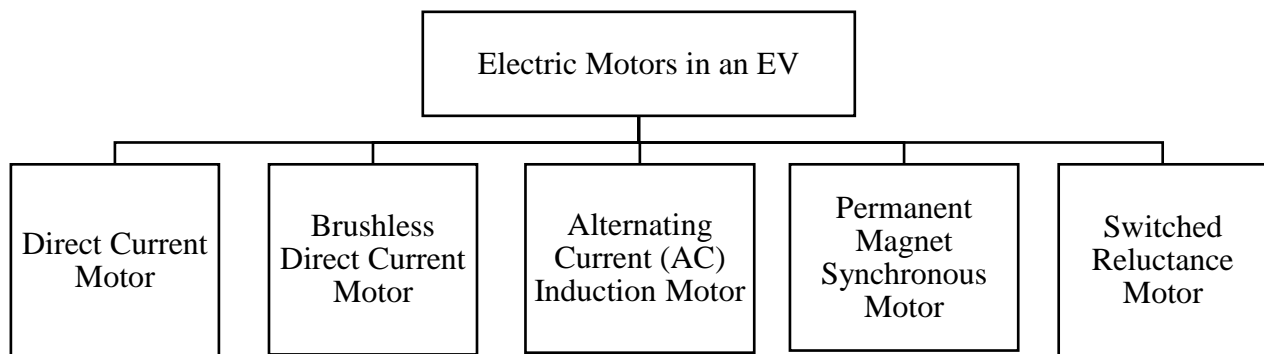


**Figure 4 Types of Electric Motor in an EV**

#### 1) *Direct Current Motor:*

DC motor technology is becoming phased out for EV application due to a key drawback of high maintenance arising from its carbon brushes/commutators needing electrical contact and over time, wear off. Apart from these, they can provide high starting torque, handle sudden increase in load, low cost, simple construction and easy to control.

#### 2) *Brushless Direct Current Motor:*

Brushless DC motor overcomes the inherent weakness of DC motor, the need for electrical contact via carbon brushes/commutator. It does away with the commutator, by having the windings on the stator and the permanent magnet on the rotor; as such, no need for carbon brushes. It also can provide high starting torque, handle sudden increase in load, low cost, simple construction, easy to control and low maintenance.

#### 3) *Alternating Current (AC) Induction Motor:*

AC induction motor also referred to asynchronous induction motor are used in EV due to their high efficiency, good speed control and low maintenance due to the absence of a commutator.

They occur in construction as either squirrel cage or wound type AC induction motors. The operation of this motor is such that, a current through rotor windings induces a magnetic field, which can interact with the magnetic field of the stator to produce a force on the rotor, causing rotation. AC induction motor

4) *Permanent Magnet Synchronous Motor:*

Permanent magnet synchronous motor (PMSM) are compact, have a high power-to-weight ratio, provide high starting torque, very stable in operation, and low maintenance. As such, widely used in various EVs such as light vehicles and buses. They occur in construction as either surface PMSM or internal PMSM. The operation of this motor is such that, the interaction of the rotating magnetic field of the stator and the constant magnetic field of the rotor formed from permanent magnet located in the rotor (i.e. surface or internal construction), producing mechanical rotation of the rotor. The key difference of a PMSM and an AC induction motor is the rotor construction.

5) *Switched Reluctance Motor:*

Switched reluctance motor is gaining adoption in EV due to their high efficiency, reliability, wide speed range, good controllability, and simple construction. Based on construction, the following configurations are applied such as singly salient and doubly salient constructions. The operation of this motor is such that, the rotor has salient poles and a cage so that it starts like an induction motor, and runs like a synchronous motor.

### *1.2.3 Power Electronics*

The power electronics in EVs as shown in Figure 5 consists of converter/inverter components and protection components. In general, they are responsible for power exchanges between EV powertrain sub-systems, such as: battery, battery management system (BMS), electric motor, and electric accessories. Converter/inverter components enable electrical power conversion by periodically fast switching available power source on and off with the use of semiconductor devices such as field-effect transistors (FETs), insulated gate bipolar transistors (IGBTs), etc. acting as switches, and energy storage devices e.g. inductors and capacitors used to store energy to filter the sharp-edged waveforms created by the fast switching operation [3]. On the other hand, protection components such as transformers are used to provide isolation, safety, and voltage/current conversions.

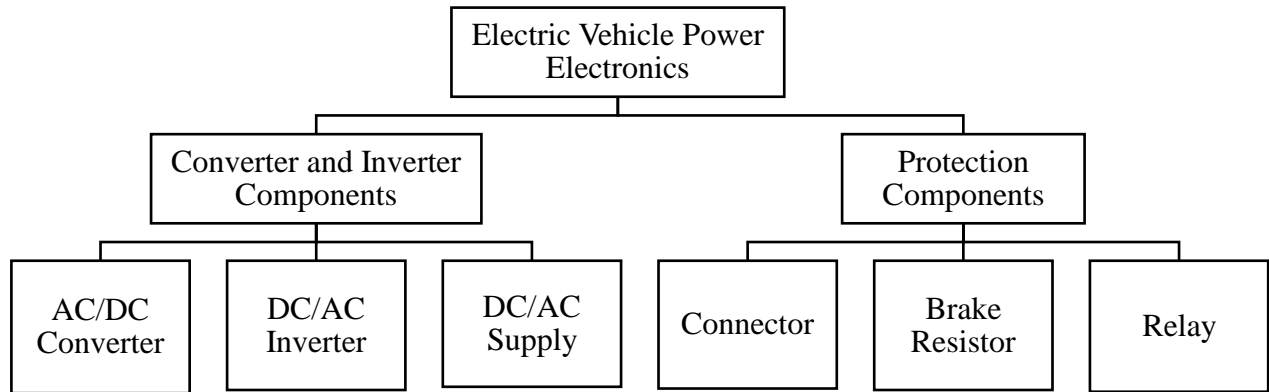


**Figure 5 Classification of Electric Vehicle Power Electronics**

## 2.0 Battery Fault Diagnosis

Failures in the battery as an energy source for EV's can have detrimental economic effect as well impact on its environmental sustainability. At the beginning, battery fault detection focused on monitoring over heating, over current and over voltage; however, with advances in battery technology, fault detection and isolation techniques have moved on.

Generally, faults in batteries can be categories as follows [5]:

- 1) *Battery Temperature Fault*: There is a minimum and maximum working temperature range for batteries (5 °C – 45 °C) [6]. When a battery operates out of this temperature range it produces under temperature fault and over temperature fault.
- 2) *Battery Current Fault*: This fault occurs in batteries due to the presence of a short circuit.
- 3) *Battery Voltage Fault*: In a battery, this fault manifests as: low voltage fault, over voltage fault, high voltage loop fault, and high voltage insulation fault.
- 4) *Battery State of Charge (SOC) Fault*: This is a fault in battery charging. It manifests as: pre-charge fault, over charging fault and over discharging fault.

### 2.1 Battery Management System (BMS)

BMS are electronic control circuits that monitors and regulate battery charging and discharging. As shown in Figure 6, the BMS must be able to satisfy the following critical functions [7]:

- 1) *Battery Protection*:

It is important for EV batteries to operate within pre-defined safe limits to ensure the safety of the user as well as the vehicle [6]. The BMS regularly monitors the battery parameters

(temperature, current and voltage) to ensure they are within safe working limits (i.e. cell voltage at full charge, 4 V, and, cell voltage at full discharge, 2 V). To prevent overheating in a Li-ion battery due to overcharging, the BMS would monitor both the cell and pack voltages to control the supply current. Another protective feature of the BMS, it ensures complete isolation of the battery pack high voltage from the chassis.

2) *Battery Monitoring:*

The BMS estimates the state of charge (SOC) and state of health (SOH) using battery parameters (temperature, current and voltage). SOC refers to the available energy in the battery, and indicates a vehicle's range on a single charge. On the other hand, SOH refers to a battery's current condition as compared to its original state. SOH also indicates a battery's suitability for application. Additionally, BMS monitors for anomalies in battery parameters (temperature, current and voltage) and trigger fail-safe or corrective actions to protect the health of the battery.

3) *Battery Optimisation:*

Batteries such as Li-ion operate optimally when SOC is maintained in practical applications within minimum 15% SOC and maximum 50% SOC battery charge profile [8]. Although, a battery can achieve 0% SOC, which is fully discharged and 100% SOC which is fully charged. This is important, as over charging and over discharging causes degradation of battery charge capacity and duration of useable life. As such, during charging, the BMS estimates the safe charge input current and communicates such to the on-board charger during AC charging or electric vehicle supply equipment (EVSE) for DC charging. Also, during discharging, the BMS prevent very low cell voltage and communicates continuously with the motor controller to avoid this. Another optimisation function of the BMS is cell balancing. Individual cells in the battery pack overtime can develop differences in capacity (i.e. cell voltage), this worsens with each discharge and charge cycle. This imbalance in cell voltage limits the amount of energy that can be discharged from the battery, and also how much the battery pack can be charged. Hence, cell balancing ensures battery cells are maintained at equal voltage levels and optimises charge capacity utilisation of the battery pack.

4) *Communication:*

BMS communicates with other electronic communication units (ECU) in the vehicle to ensure a fault free operation such as communicating battery parameters to the motor controller during

discharging or during charging, communicating safe input current with the on-board charger (AC charging) or electric vehicle supply equipment (DC charging).

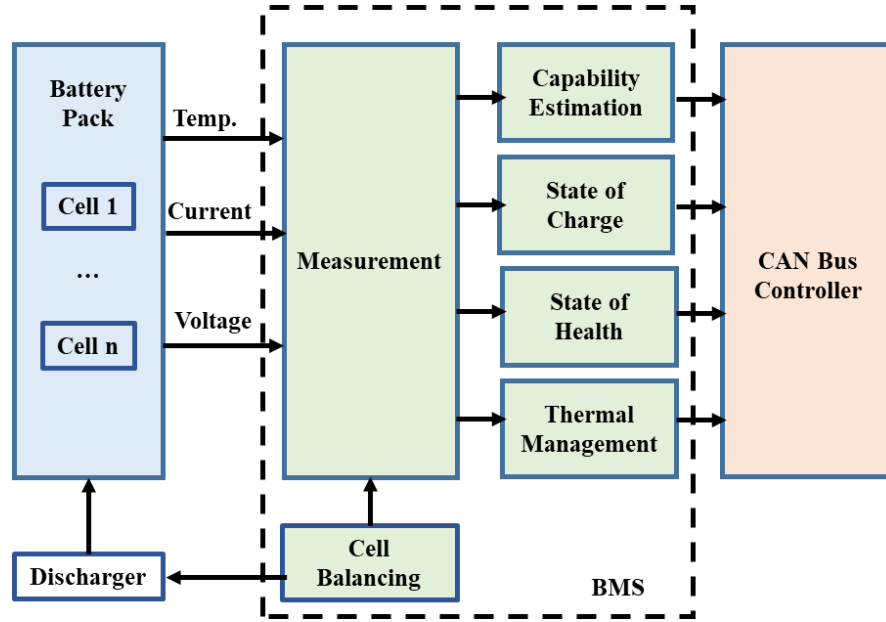


Figure 6 Schematic of battery management system [7]

## 2.2 Model-Based FDI Approach

### 2.2.1 Battery Modelling

A battery represents a nonlinear thermal-electrochemical system. Battery models help answer the following questions: what is the battery state of charge, state of health, and performance and lifespan trade-offs due to chemical and mechanical degradation of the battery caused by environment and cycling [9,10]. Two approaches are generally applied for battery modelling are [11]: equivalent circuit model and electrochemical model. The equivalent circuit battery model refers to a simplified theoretical circuit model that retains all the electrical properties of the battery. Several such models have been proposed [11–13]: Rint battery model, Thevenin battery model, PNGV battery model [14], Dual Polarisation battery model and RC battery model. On the other hand, the complex electrochemical model [15] would consider the battery cell electrical dynamics at the molecular level.

#### 1) Rint Battery Model:

The Rint battery model as shown in Figure 7, considers the battery open-circuit voltage as an ideal voltage source and the battery internal resistance as a resistor [11,12]. Both parameters,

open-circuit voltage and internal resistance, are function of SOC, SOH and temperature.  $I_L$  is load current with a positive value at discharging and a negative value at charging,

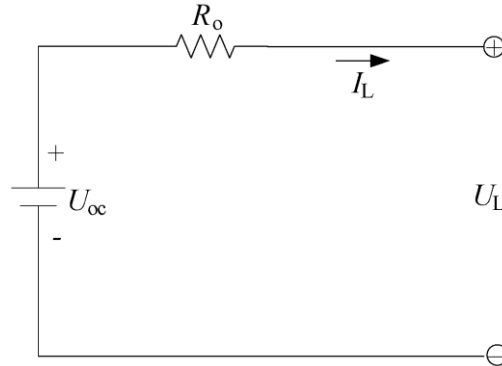


**Figure 7 Rint battery model** [11,12]

Applying circuit theory to Figure 7, the following governing equation applies [12]:

$$U_L = U_{oc} - I_L R_o \quad (1)$$

where  $U_{oc}$  is battery open-circuit voltage,  $R_o$  is battery internal resistance,  $U_L$  is battery terminal voltage and  $I_L$  is load current.

2) *Thevenin Battery Model:*

Thevenin battery model is an extension of the Rint battery model. It addresses the transient effect on the battery due to charging and discharging. This is implemented in the model by incorporating a parallel RC network in series with the Rint battery model as shown in Figure 8. The model consist of the open-circuit voltage  $U_{oc}$ , battery internal resistances (ohmic resistance  $R_o$  and polarisation resistance  $R_{th}$ ) and equivalent battery capacitance  $C_{th}$ .

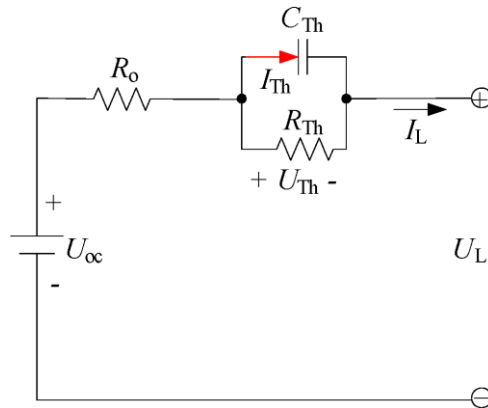


**Figure 8 Thevenin battery model** [12]

Applying circuit theory to Figure 8, the following governing equation applies [12]:

$$\dot{U}_{TH} = -\frac{U_{TH}}{R_{TH}C_{TH}} + \frac{I_L}{C_{TH}} \quad (2)$$

$$U_L = U_{OC} - U_{TH} - I_L R_o \quad (3)$$

where  $U_{oc}$  is battery open-circuit voltage,  $U_L$  is battery terminal voltage and  $I_L$  is load current.

### 3) PNGV Battery Model:

PNGV battery model as shown in Figure 9 is an extension of Thevenin battery model. It addresses the changing open-circuit battery voltage due to time related accumulation of load current. This is implemented by incorporating a capacitor in series to the Thevenin battery model.

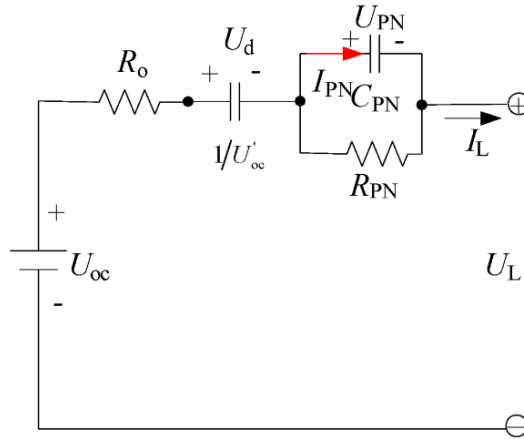


**Figure 9 PNGV battery model**

Applying circuit theory to Figure 9, the following governing equation applies [12]:

$$\dot{U}_d = U'_{OC} I_L \quad (4)$$

$$\dot{U}_{PN} = \frac{U_{PN}}{R_{PN}C_{PN}} + \frac{I_L}{C_{PN}} \quad (5)$$

$$U_L = U_{OC} - U_d - U_{PN} - I_L R_o \quad (6)$$

where  $U_{oc}$  is battery open-circuit voltage,  $U_L$  is battery terminal voltage,  $I_L$  is load current, battery internal resistances (ohmic resistance  $R_o$  and polarisation resistance  $R_{PN}$ ),  $U_d$  is the voltage across series capacitor  $1/U'_{oc}$  and  $U_{PN}$  is voltage across polarisation capacitor  $C_{PN}$  and  $I_{PN}$  is the output current from  $C_{PN}$ .

### 4) Dual Polarisation (DP) Battery Model:

DP battery model extends the Thevenin battery model by considering the effect of concentration polarisation as well as the electrochemical polarisation. This is implemented by incorporating an RC parallel network in series with the Thevenin battery model. The DP

battery model as shown in Figure 10 consist of the open-circuit battery voltage  $U_{oc}$ , battery ohmic resistance  $R_o$ , battery polarisation resistances (i.e. effective electro-chemical polarisation resistance  $R_{pa}$  and effective concentration polarisation resistance  $R_{pc}$ ), and polarisation capacitance (i.e. electro-chemical polarisation capacitance  $C_{pa}$  which accounts for charging and discharging transient effects and the concentration polarisation capacitance  $C_{pc}$ ).

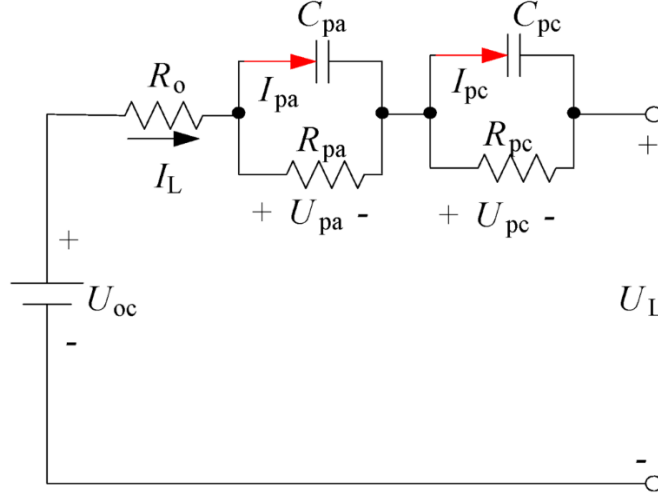


**Figure 10 DP battery model [12]**

$$\dot{U}_{pa} = -\frac{U_{pa}}{R_{pa}C_{pa}} + \frac{I_L}{C_{pa}} \quad (7)$$

$$\dot{U}_{pc} = \frac{U_{pc}}{R_{pc}C_{pc}} + \frac{I_L}{C_{pc}} \quad (8)$$

$$U_L = U_{oc} - U_{pa} - U_{pc} - I_L R_o \quad (9)$$

where  $\dot{U}_{pa}$  and  $\dot{U}_{pc}$  are derivatives of the voltage across the electro-chemical polarisation capacitor  $U_{pa}$ , and concentration capacitor  $U_{pc}$  respectively, open-circuit voltage  $U_{oc}$ , and  $I_L$  is load current.

5) *RC Battery Model:*

The RC battery model as shown in Figure 11 considers a battery as two capacitor (surface capacitor  $C_c$  and bulk capacitor  $C_b$ ), and three resistors (terminal resistor  $R_t$ , end resistor  $R_e$ , capacitor resistor  $R_c$ ) [11,12]. Here, surface capacitor  $C_c$  represents the small capacitive surface effect of the battery, and the bulk capacitor  $C_b$  represents battery charge storage.

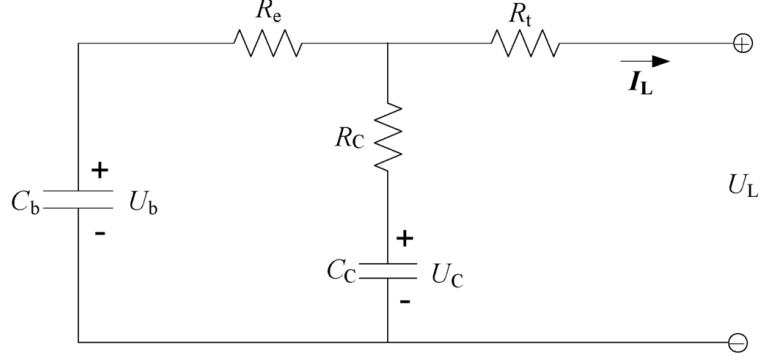


**Figure 11 RC battery model [11,12]**

Applying circuit theory to Figure 11, the following governing equation applies [11,12]:

$$\begin{bmatrix} \dot{U}_b \\ \dot{U}_c \end{bmatrix} = \begin{bmatrix} \frac{-1}{C_b(R_e + R_c)} & \frac{1}{C_b(R_e + R_c)} \\ \frac{1}{C_c(R_e + R_c)} & \frac{-1}{C_c(R_e + R_c)} \end{bmatrix} \begin{bmatrix} U_b \\ U_c \end{bmatrix} + \begin{bmatrix} \frac{-R_c}{C_b(R_e + R_c)} \\ \frac{-R_e}{C_b(R_e + R_c)} \end{bmatrix} [I_L] \quad (10)$$

$$[U_L] = \begin{bmatrix} \frac{R_c}{(R_e + R_c)} & \frac{R_e}{(R_e + R_c)} \end{bmatrix} \begin{bmatrix} U_b \\ U_c \end{bmatrix} + \left[ -R_t - \frac{R_c R_e}{(R_e + R_c)} \right] [I_L] \quad (11)$$

where  $\dot{U}_b$  and  $\dot{U}_c$  are derivatives of the bulk capacitor voltage  $U_b$  and surface capacitor voltage  $U_c$ , and  $I_L$  is load current.

6) *Thermal-Electrochemical Battery Model:*

Thermal-electrochemical battery model as shown in Figure 12 couples the battery cell thermal energy equation with the multiphase micro-macroscopic electrochemical model via the heat generation and temperature-dependent physicochemical properties such as diffusion coefficient and ionic conductivity of the electrolyte [15,16]. Electrochemical battery models are capable of predicting both the spatial and average temperature in the battery cell, cell charge and discharge efficiencies, cell pressures, dynamic potential and current curves, and active material utilisation [9,15,16].

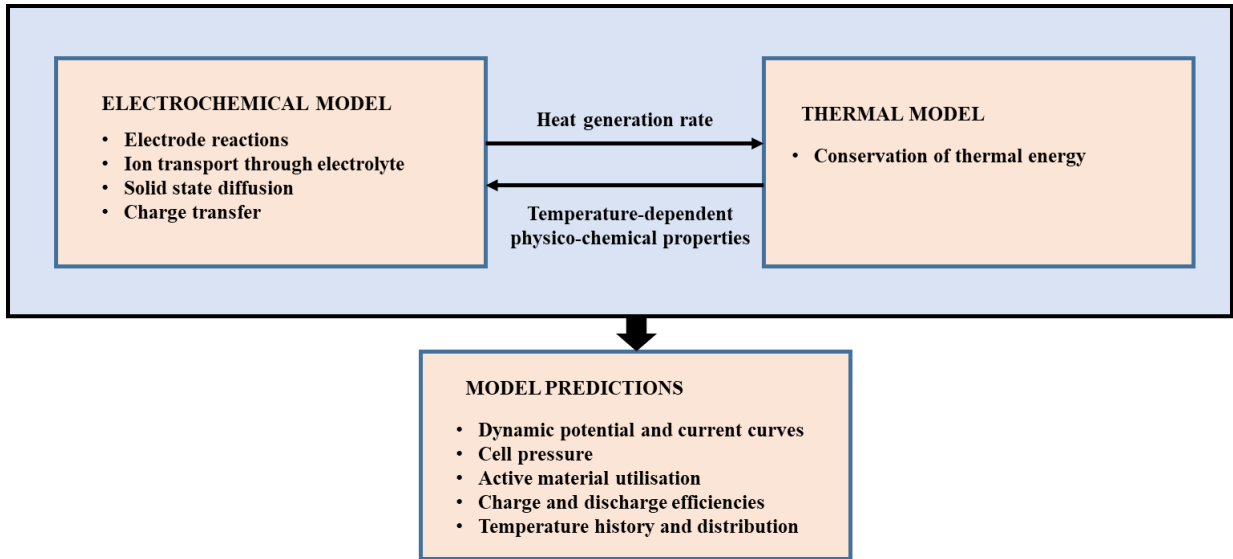


**Figure 12 Schematic of thermal-electrochemical [15]**

### 2.3 Signal Processing-Based FDI Approach

Although the BMS using measurement of battery voltage, current and temperature can estimate the batteries state of charge and health, limitation exist regarding individual fault type diagnostic and accuracy in state estimation [5]. For this application, Figure 13 shows an advanced battery diagnostics system using signal processing-based. This system integrates both hardware components (i.e. signal modulation circuit and data acquisition card), as well as a software components (i.e. acquisition module and management module). The hardware components monitor the battery parameters (i.e. voltage, current and temperature) and modulate the signals for storage by the acquisition card. Within the acquisition and management modules, software apply signal processing-based approach on the stored data to perform performance and diagnostic checks. Some of these techniques are presented below.

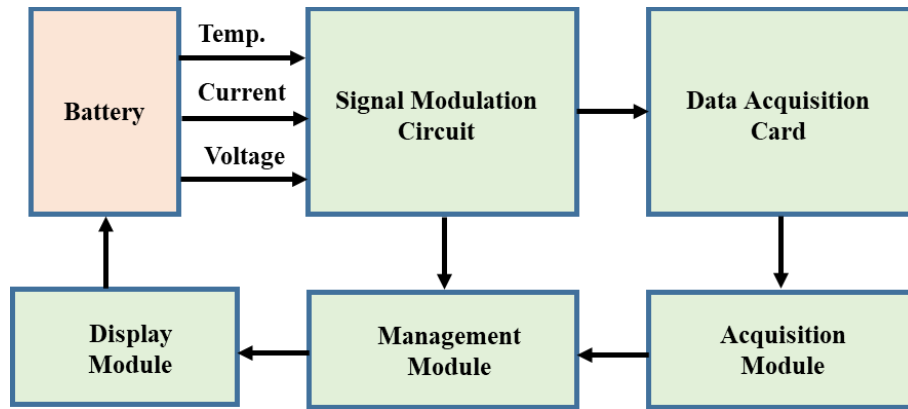


**Figure 13 Schematic of Advanced Battery Diagnostic System [5]**

### 2.3.1 State of Charge (SOC) Estimation

Battery SOC represent its remaining charge capacity. Mathematically, SOC is a ratio between the battery's current capacity to its nominal capacity [17]. It is an important parameter required by battery management system for effective control of the battery. Chang [17] reviewed various approaches for SOC estimation. Broadly, there are four categories of SOC estimation methods: direct measurement methods, book keeping estimation, adaptive systems, and hybrid methods. In the adaptive systems and hybrid methods, signal processing-based techniques such as Kalman filter [18], extended Kalman filter [19,20] and unscented Kalman filter [21,22] are important and provide improvements in accuracy.

### 2.3.2 State of Health Estimation

Battery SOH is an indication of the ability of a battery to store and release a charge as compared to a new battery. Monitoring the SOH of a battery is important for prolonging the battery lifetime. Noura [23] provides a review of methods for estimating the SOH of batteries. As shown in Figure 14, signal processing-based techniques such as Kalman filter, extended Kalman filter and unscented Kalman filter as applied in the adaptive systems approach are relevant for accurate battery SOH estimation [23–25].

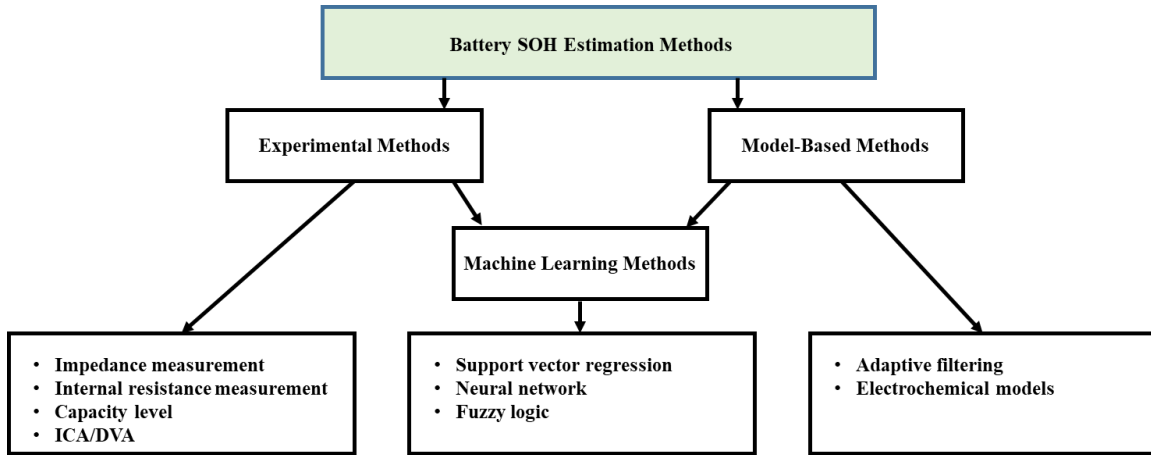


Figure 14 Overview of battery SOH estimation methods [23]

### 3.0 Electric Motor Fault Diagnosis

#### 3.1 Electric Motor Faults

Although electric motor types are varied in construction, they all have the following components: stator, rotor, and bearings as shown in Figure 15. As such, a common trend can be observed regarding fault occurrence.

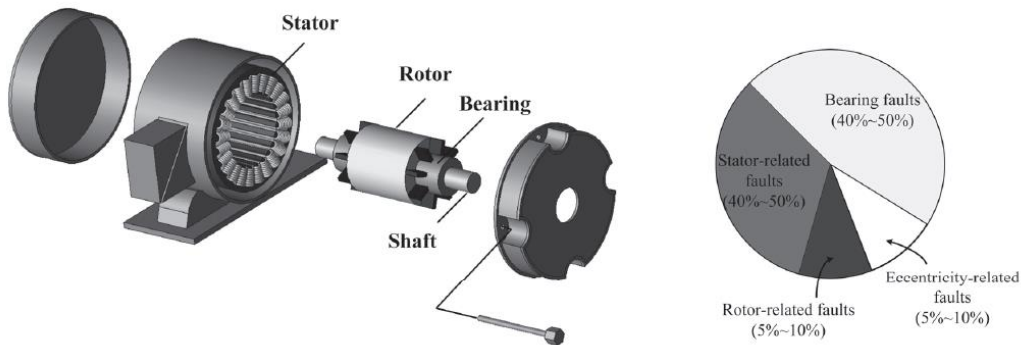


Figure 15 Parts of an electric motor and failure mode [5]

Generally, faults in an electric motor can be grouped as [26]:

##### 3.1.1 Mechanical Fault

These are faults that affect the integrity of the bearing and the eccentricity of the rotor in the stator. Bearing related fault can manifest as inner and outer bearing race defects, rolling-element defect and cage defect. Eccentricity-related faults can be due to bend shaft, air gap irregularity, etc.

### 3.1.2 Electrical Fault

Electrical fault is associated with faults in the rotor and stator. Rotor related fault can manifest as broken rotor bar, short circuit rotor winding, cracked rotor end ring, etc. Stator related fault can occur as open circuit stator winding, short circuit stator winding, and abnormal connection of stator winding.

## 3.2 Signal Processing-Based FDI Approach

### 3.2.1 Motor Current Signature Analysis (MSCA)

MSCA is a fault detection and isolation technique applicable for induction motors [27]. The concept has its origin dating back to 1970 in the nuclear industry where it was applied for monitoring the health of electric motor which were located in inaccessible and often hazardous conditions [27]. In recent times, MSCA is also applied to EVs and other industries to monitor the health of electric motors [28–30]. MSCA is quite advantageous, as it does not interrupt the operation of the electric motors. As shown in Figure 16, MSCA acquires the current signal (i.e. stator current) from one phase of the motor supply without interrupting its operation. In MSCA, the current signal is processed using a signal-processing technique such as Fast Fourier Transform (FFT) to obtain the frequency spectrum also called current spectrum. MSCA uses the current spectrum of the electric motor for locating fault frequencies. As shown in Figure 17, the current spectrum of the electric motor with a fault is different from the current spectrum of a healthy motor.

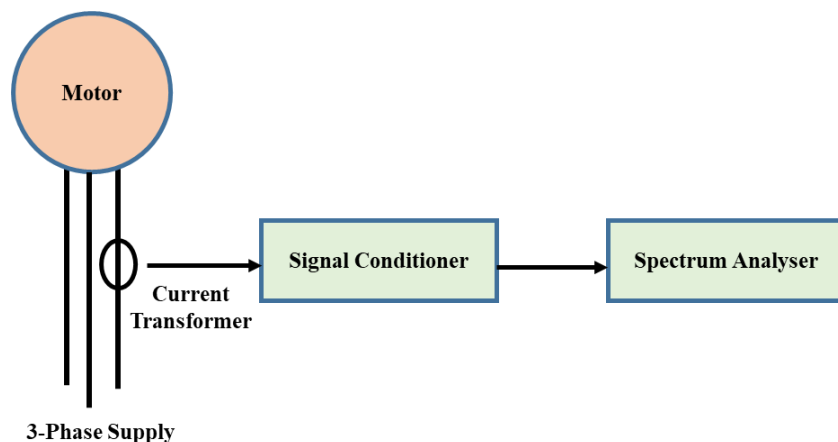


Figure 16 Overview of MSCA approach [27]

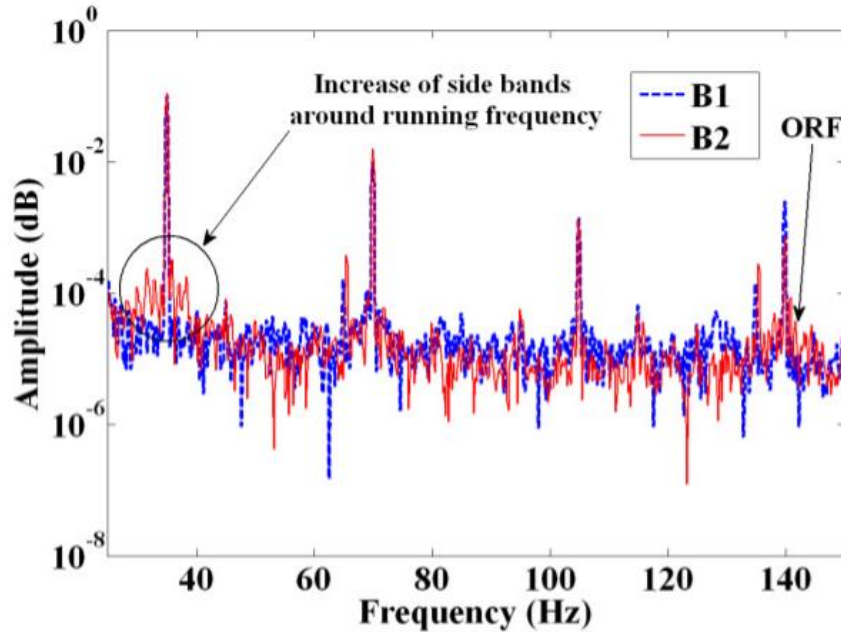


Figure 17 Current spectrum from MSCA of a healthy electric motor (B1) and faulty electric motor with damaged bearings (B2) [31]

With MSCA, the following faults in an electric motor are detectable [27]:

1) *Air Gap Eccentricity:*

Air gap eccentricity occurs when the air gap between the rotor and stator in the electric motor is not uniform. This can occur due to assembly and manufacturing errors. This can take the form of the following:

- Static Eccentricity: Occurs when the rotor geometrical and rotational centres are identical; however, different from the stator geometrical centre. This can happen due to manufacturing tolerances not meet.
- Dynamic Eccentricity: occurs when the rotor geometrical centre does not coincide with its rotational centre.
- Mixed Eccentricity: this is a combination of both the static and dynamic eccentricities.

In determination of static eccentricity using MSCA, sidebands would occur around the eccentricity frequency  $f_{ec}$ , determined by:

$$f_{ec} = f_g \left\{ (R \pm n_d) \left( \frac{1-s}{p} \right) \pm n_{ws} \right\} \quad (12)$$

where  $f_{ec}$  is eccentricity frequency,  $f_g$  is line or supply frequency, R is number of rotor bar, s is slip, p is number of pole pairs,  $n_d = \pm 1$ , and  $n_{ws} = 1, 3, 5, \dots$

Slip (s) is determined by:

$$s = \frac{N_s - N_r}{N_s} \quad (13)$$

where  $N_s$  is rotor speed and  $N_r$  is rotor synchronous speed.

Also, static eccentricity can occur as sideband around the centre frequency  $f_c$  given below and also shown in Figure 18

$$f_c = Rf_g \quad (14)$$

where  $f_g$  is supply frequency, and R is number of rotor bar.

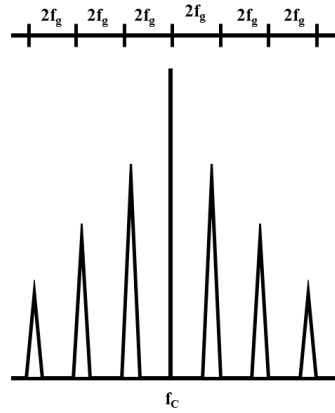


**Figure 18 Air gap static eccentricity current spectrum [27]**

Furthermore, the occurrence of air gap dynamic eccentricity is detected by further harmonics to the current spectrum as shown in Figure 19. These new harmonics are modulated by the mechanical rotor frequency  $f_g$ .

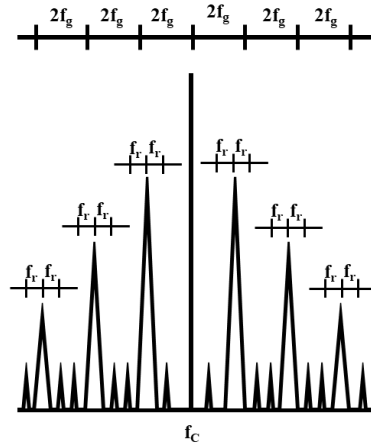


**Figure 19 Air gap dynamic eccentricity current spectrum [27]**

2) *Broken Rotor Bar:*

Broken rotor bar can occur in induction motors due to arduous duty cycles. In themselves, they would not cause failure of the induction motor; however, they can create secondary damage e.g. broken rotor bar parts can damage the winding. With MCSA, broken rotor bar fault can be detected in the current spectrum by the presence of the broken rotor bar frequency component, determined by [27]:

$$f_{brb} = f_g \left[ k \left( \frac{1-s}{p} \right) \pm s \right] \quad (15)$$

where  $f_{brb}$  is broken rotor bar frequency,  $f_g$  is line or supply frequency,  $p$  is pole pairs,  $s$  is slip, and  $k = 1, 2, 3 \dots$ .

3) *Bearing Fault:*

Bearing damage in electric motors is primarily caused by misalignment especially during installation. With MSCA, bearing faults is detected by the presence of bearing fault frequency components  $f_0$  and  $f_1$  in the current spectrum. For bearings with 6-12 rolling elements, these frequency components can be determined as follows [27]:

$$f_o = 0.4n f_{rm} \quad (16)$$

$$f_1 = 0.6n f_{rm} \quad (17)$$

where  $f_o$  is lower frequency,  $f_1$  is upper frequency,  $n$  is number of rolling elements, and  $f_{rm}$  is the mechanical rotational frequency of the rotor.

4) *Shorted Turns-In Stator Windings:*

Shorted stator winding fault is very common fault in induction motors. The stator current can be continuously monitored in order to predict incipient fault in the stator windings. In MSCA, the shorted turns-in stator windings fault can be detected by the presence of shorted stator windings frequency component determined by [27]:

$$f_{st} = f_g \left[ \frac{n}{p} (1-s) \pm k \right] \quad (18)$$

where  $f_{st}$  is shorted stator winding frequency,  $f_g$  is line or supply frequency,  $n$  is number of rolling elements,  $p$  is pole pairs,  $s$  is slip and  $k = 1, 2, 3 \dots$

5) *Load Effects:*

During the operation of an electric motor, as a result of duty cycle demand, there can be variation or fluctuation in the transmitted torque. This load effect can also be monitored by

MSCA. Using MSCA, variability in torque can be detected by the presence of the following frequency component in the current spectrum, determined as such [27]:

$$f_{load} = f_s \pm m f_r = f_s \left[ 1 \pm m \left( \frac{1-s}{p} \right) \right] \quad (19)$$

where  $f_s$  is line or supply frequency,  $f_r$  is mechanical rotational frequency,  $p$  is number of pole pairs,  $s$  is slip and  $km = 1,2,3 \dots$

#### 4.0 Power Electronics Fault Diagnosis

The reliability of power converter/inverter components depends primarily on the endurance of its main component, the power switches [32]. Although there varied types of power switches such as: thyristor, gate turn-off thyristor (GTO), power bipolar-junction transistor (BJT), power metal-oxide field effect transistor (MOSFET), insulated gate bipolar transistor (IGBT), static induction transistor (SIT), static induction thyristor (SITH), MOS controlled thyristor (MCT), and MOS turn-off thyristor (MTO); for EV power converter/inverter, IGBT is the widely adopted switching technology [3,32,33].

For power switching devices, the most common types of faults are [32]:

- 1) Open switch fault
- 2) Short switch fault

#### 4.1 Signal Processing-Based FDI Approach

##### 4.1.1 Open Switch Fault

An open switch fault in an IGBT can be due to a break of its bond wires or fault in the gate drive. This results in a DC offset in the faulty phase/leg. Figure 20 shows an example of an open switch fault in  $S_{ap}$  a three-phase two leg inverter controlling an AC motor. As the IGBT with the open switch fault would not turn ON, in the case of motor operation, the current in that phase becomes zero for a half-cycle, either positive or negative half-cycle depending on whether it is upper IGBT or lower IGBT. This behaviour results in the DC offset observed in practice from the faulty phase.

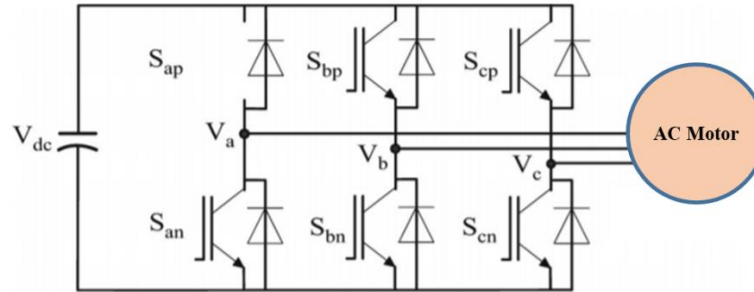


**Figure 20 three-phase two-level inverter with IGBT open switch fault at  $S_{ap}$  [32]**

To detect open switch fault in power drives, several approaches are reported in literature [5,32,34–37]; however, two broad methods are evident [32]: voltage sensor measurements [35] and software defined-techniques [36,37].

Voltage sensor measurement techniques are fast acting and require short detection time. However, they require additional voltage sensor to insert into the system. Depending on the location of insertion of the voltage sensor, the following voltage measurement indicators are relevant for power drive open switch fault diagnosis [32,35]:

- Inverter pole voltage measurement
- Machine phase voltage measurement
- System line voltage measurement
- Machine neutral voltage measurement

Software defined-techniques do not require additional voltage sensors; although they require a longer detection time. In this category, various techniques for tracking the current vector trajectory [36,38] and 3-phase current mean value [39] as indicators for open switch fault in power drives has been proposed. Table 2 provides an overview of techniques used for detecting open switch fault in power drives [5].

**Table 2 Summary of power drive open switch fault detection [5]**

Fault	Symptoms	Fault Indicator	Approach	Comments
Open switch fault	DC current offset	Current vector trajectory	Park's method	Load dependent
			Normalised DC current method	Complicated
			Modified normalised DC current method	High efficient
		3-phase current mean value	Wavelet-neural network method	High cost, intelligent
			Current deviation method	High implementation effort
		Voltage	Voltage comparison in time domain	Extra sensor needed
	Voltage sensing by lower switch	Quick detection		

#### 4.1.2 Short Switch Fault

A short switch fault in an IGBT may be due to the malfunctioning of the gate drive or permanent damage to the IGBT. This results in practice to a non-zero DC current in the shortened phase/leg. Short switch fault results very quickly in the failure of the e-drive, as such isolating the shortened phase with approach such as a fast-acting fuse or field programmable gate array, etc. is required especially for fault tolerant mode of operation. Figure 21 shows an example of a short switch fault in  $S_{ap}$  a three-phase two leg inverter controlling an AC motor. When the IGBT detects the short circuit fault, all the IGBTs are turned OFF by hardware protection. In the event of IGBT permanent damage, its corresponding phase is permanently connected to the dc link positive bus or negative bus depending on upper IGBT or lower IGBT is damaged. Provided the machine is operational, current flows through the shorted IGBT and remaining freewheeling diodes of the inverter.

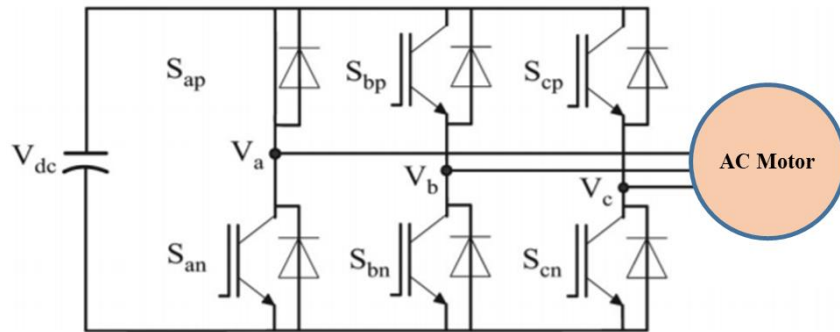


**Figure 21** three-phase two-level inverter with IGBT short switch fault at  $S_{ap}$  [32]

To detect short switch fault in power drives, the following current and voltage measurement parameters are relevant for fault diagnosis [5]:

- Phase current
- Device current
- Gate voltage

Table 3 highlight various techniques for detecting short switch circuit.

**Table 3** Summary of power drive short switch fault diagnosis [5]

Fault	Symptoms	Fault Indicator	Approach	Comments
Short switch fault	Non-zero DC current component	Phase current	Average current Park's vector approach	No protection
		Device current	Current mirror method	High cost
		Gate Voltage	Protection by gate voltage limiting	Inaccurate detection
			Gate voltage sensing method	Complicated
			Two-step gate pulse	Reliable
		Voltage and time criterion	Fast reaction, fault tolerant	

## 5.0 Conclusions

In this chapter, an overview of EV powertrain technologies and various configuration has been identified. Recent research on fault detection for powertrain components such as battery, electric motor and power electronics have also been discussed, with emphasis on the application of various model-based and signal processing-based fault detection and isolation approaches relevant for EVs.

## References

1. Un-Noor, F., Padmanaban, S., Mihet-Popa, L., Mollah, M.N., and Hossain, E. (2017) A Comprehensive Study of Key Electric Vehicle (EV) Components, Technologies, Challenges, Impacts, and Future Direction of Development. *Energies* , **10** (8).
2. Chan, C.C. (2002) The state of the art of electric and hybrid vehicles. *Proc. IEEE*, **90** (2), 247–275.
3. Chau, K., and Wang, Z. (2005) Overview of power electronic drives for electric vehicles. *HAIT J. Sci. Eng. B*, **2** (5–6), 737–761.
4. Landi, B.J., Ganter, M.J., Cress, C.D., DiLeo, R.A., and Raffaele, R.P. (2009) Carbon nanotubes for lithium ion batteries. *Energy Environ. Sci.*, **2** (6), 638–654.
5. Lin, F., Chau, K.T., Chan, C.C., and Liu, C. (2013) Fault Diagnosis of Power Components in Electric Vehicles. *J. Asian Electr. Veh.*, **11** (2), 1659–1666.
6. Ma, S., Jiang, M., Tao, P., Song, C., Wu, J., Wang, J., Deng, T., and Shang, W. (2018) Temperature effect and thermal impact in lithium-ion batteries: A review. *Prog. Nat. Sci. Mater. Int.*, **28** (6), 653–666.
7. Buccolini, L., Ricci, A., Scavongelli, C., DeMaso-Gentile, G., Orcioni, S., and Conti, M. (2016) Battery Management System (BMS) simulation environment for electric vehicles. *2016 IEEE 16th Int. Conf. Environ. Electr. Eng.*, 1–6.
8. Wikner, E., and Thiringer, T. (2018) Extending battery lifetime by avoiding high SOC. *Appl. Sci.*, **8** (10).
9. Li, C., Cui, N., Wang, C., and Zhang, C. (2021) Simplified electrochemical lithium-ion battery model with variable solid-phase diffusion and parameter identification over wide temperature range. *J. Power Sources*, **497**, 229900.
10. Grolleau, S., Delaille, A., and Gualous, H. (2013) Predicting lithium-ion battery degradation

- for efficient design and management. *World Electr. Veh. J.*, **6** (3), 549–554.
11. Xu, J., and Cao, B. (2015) Battery Management System for Electric Drive Vehicles – Modeling, State Estimation and Balancing, in *New Applications of Electric Drives* (eds.Chomat, M.), InTechOpen.
  12. He, H., Xiong, R., and Fan, J. (2011) Evaluation of Lithium-Ion Battery Equivalent Circuit Models for State of Charge Estimation by an Experimental Approach. *Energies* , **4** (4).
  13. Johnson, V.H. (2002) Battery performance models in ADVISOR. *J. Power Sources*, **110** (2), 321–329.
  14. Liu, X., Li, W., and Zhou, A. (2018) PNGV Equivalent Circuit Model and SOC Estimation Algorithm for Lithium Battery Pack Adopted in AGV Vehicle. *IEEE Access*, **6**, 23639–23647.
  15. Gu, W.B., and Wang, C.Y. (2000) Thermal-Electrochemical Modeling of Battery Systems. *J. Electrochem. Soc.*, **147** (8), 2910.
  16. Anwar, S., Zou, C., and Manzie, C. (2014) Distributed Thermal-Electrochemical Modeling of a Lithium-Ion Battery to Study the Effect of High Charging Rates. *IFAC Proc. Vol.*, **47** (3), 6258–6263.
  17. Chang, W.-Y. (2013) The State of Charge Estimating Methods for Battery: A Review. *ISRN Appl. Math.*, **2013**, 953792.
  18. Yatsui, M.W., and Bai, H. (2011) Kalman filter based state-of-charge estimation for lithium-ion batteries in hybrid electric vehicles using pulse charging. *2011 IEEE Veh. Power Propuls. Conf.*, 1–5.
  19. Xu, L., Wang, J., and Chen, Q. (2012) Kalman filtering state of charge estimation for battery management system based on a stochastic fuzzy neural network battery model. *Energy Convers. Manag.*, **53** (1), 33–39.
  20. Barbarisi, O., Vasca, F., and Glielmo, L. (2006) State of charge Kalman filter estimator for automotive batteries. *Control Eng. Pract.*, **14** (3), 267–275.
  21. Zhang, J., and Xia, C. (2011) State-of-charge estimation of valve regulated lead acid battery based on multi-state Unscented Kalman Filter. *Int. J. Electr. Power Energy Syst.*, **33** (3), 472–476.
  22. Tong, B., Wang, G., and Sun, X. (2014) Investigation of the Fluid-Solid Thermal Coupling for Rolling Bearing under Oil-Air Lubrication. *Adv. Mech. Eng.*, **7** (2), 835036.

23. Noura, N., Boulon, L., and Jemeï, S. (2020) A review of battery state of health estimation methods: Hybrid electric vehicle challenges. *World Electr. Veh. J.*, **11** (4), 1–20.
24. Shen, P., Ouyang, M., Lu, L., Li, J., and Feng, X. (2018) The Co-estimation of State of Charge, State of Health, and State of Function for Lithium-Ion Batteries in Electric Vehicles. *IEEE Trans. Veh. Technol.*, **67** (1), 92–103.
25. Kim, J., and Cho, B.H. (2011) State-of-Charge Estimation and State-of-Health Prediction of a Li-Ion Degraded Battery Based on an EKF Combined With a Per-Unit System. *IEEE Trans. Veh. Technol.*, **60** (9), 4249–4260.
26. Benbouzid, M.E.H. (2000) A review of induction motors signature analysis as a medium for faults detection. *IEEE Trans. Ind. Electron.*, **47** (5), 984–993.
27. Miljkovic, D. (2015) Brief review of motor current signature analysis. *HDKBRInfo Mag.*, **5**, 14–26.
28. Praneeth, A.V.J.S., and Williamson, S.S. (2017) Algorithm for prediction and control of induction motor stator interturn faults in electric vehicles. *2017 IEEE Transp. Electr. Conf. Expo*, 130–134.
29. Fontes, A.S., Cardoso, C.A. V, and Oliveira, L.P.B. (2016) Comparison of techniques based on current signature analysis to fault detection and diagnosis in induction electrical motors. *2016 Electr. Eng. Conf.*, 74–79.
30. Thomson, W.T., and Culbert, I. (2017) Motor Current Signature Analysis for Induction Motors, in *Current Signature Analysis for Condition Monitoring of Cage Induction Motors: Industrial Application and Case Histories*, IEEE, pp. 1–37.
31. Singh, S., Kumar, A., and Kumar, N. (2014) Motor Current Signature Analysis for Bearing Fault Detection in Mechanical Systems. *Procedia Mater. Sci.*, **6**, 171–177.
32. Errabelli, R.R., and Mutschler, P. (2012) Fault-Tolerant Voltage Source Inverter for Permanent Magnet Drives. *IEEE Trans. Power Electron.*, **27** (2), 500–508.
33. Rodriguez, M.A., Claudio, A., Theilliol, D., and Vela, L.G. (2007) A New Fault Detection Technique for IGBT Based on Gate Voltage Monitoring. *2007 IEEE Power Electron. Spec. Conf.*, 1001–1005.
34. Fuchs, F.W. (2003) Some diagnosis methods for voltage source inverters in variable speed drives with induction machines - a survey. *IECON'03. 29th Annu. Conf. IEEE Ind. Electron. Soc. (IEEE Cat. No.03CH37468)*, **2**, 1378-1385 Vol.2.

35. Ribeiro, R.L. de A., Jacobina, C.B., Silva, E.R.C. da, and Lima, A.M.N. (2003) Fault detection of open-switch damage in voltage-fed PWM motor drive systems. *IEEE Trans. Power Electron.*, **18** (2), 587–593.
36. Peugeot, R., Courtine, S., and Rognon, J.-. (1998) Fault detection and isolation on a PWM inverter by knowledge-based model. *IEEE Trans. Ind. Appl.*, **34** (6), 1318–1326.
37. Jung, S., Park, J., Kim, H., Kim, H., and Youn, M. (2009) Simple switch open fault detection method of voltage source inverter. *2009 IEEE Energy Convers. Congr. Expo.*, 3175–3181.
38. Kim, S.Y., Nam, K., Song, H., and Kim, H. (2008) Fault Diagnosis of a ZVS DC–DC Converter Based on DC-Link Current Pulse Shapes. *IEEE Trans. Ind. Electron.*, **55** (3), 1491–1494.
39. Mamat, M.R., Rizon, M., and Khanniche, M.S. (2006) Fault Detection of 3-Phase VSI using Wavelet-Fuzzy Algorithm. *Am. J. Appl. Sci.*, **3** (1 SE-Research Article).